

[C II] emission in $z \sim 6$ strongly lensed, star-forming galaxies

Kirsten K. Knudsen,¹★ Johan Richard,² Jean-Paul Kneib,^{3,4} Mathilde Jauzac,^{5,6,7}
Benjamin Clément,² Guillaume Drouart,⁸ Eiichi Egami,⁹ Lukas Lindroos¹

¹Department of Earth and Space Sciences, Chalmers University of Technology, Onsala Space Observatory, SE-43992 Onsala, Sweden

²Univ Lyon, Univ Lyon1, Ens de Lyon, CNRS, Centre de Recherche Astrophysique de Lyon UMR5574, F-69230, Saint-Genis-Laval, France

³Laboratoire d'Astrophysique, Ecole Polytechnique Fédérale de Lausanne (EPFL), Observatoire de Sauverny, CH-1290 Versoix, Switzerland

⁴Aix Marseille Université, CNRS, LAM (Laboratoire d'Astrophysique de Marseille), UMR 7326, 13388 Marseille, France

⁵Centre for Extragalactic Astronomy, Department of Physics, Durham University, Durham DH1 3LE, U.K.

⁶Institute for Computational Cosmology, Durham University, South Road, Durham DH1 3LE, U.K.

⁷Astrophysics and Cosmology Research Unit, School of Mathematical Sciences, University of KwaZulu-Natal, Durban 4041, South Africa

⁸International Centre for Radio Astronomy Research, Curtin University, Bentley, WA6102, Perth, Australia

⁹Steward Observatory, University of Arizona, 933 N. Cherry Ave, Tucson, AZ 85721, USA

Accepted XXX. Received YYY; in original form ZZZ

ABSTRACT

The far-infrared fine-structure line [C II] at 1900.5 GHz is known to be one of the brightest cooling lines in local galaxies, and therefore it has been suggested to be an efficient tracer for star-formation in very high-redshift galaxies. However, recent results for galaxies at $z > 6$ have yielded numerous non-detections in star-forming galaxies, except for quasars and submillimeter galaxies. We report the results of ALMA observations of two lensed, star-forming galaxies at $z = 6.029$ and $z = 6.703$. The galaxy A383-5.1 (star formation rate [SFR] of $3.2 M_{\odot} \text{ yr}^{-1}$ and magnification of $\mu = 11.4 \pm 1.9$) shows a line detection with $L_{[\text{C II}]} = 8.9 \times 10^6 L_{\odot}$, making it the lowest $L_{[\text{C II}]}$ detection at $z > 6$. For MS0451-H (SFR = $0.4 M_{\odot} \text{ yr}^{-1}$ and $\mu = 100 \pm 20$) we provide an upper limit of $L_{[\text{C II}]} < 3 \times 10^5 L_{\odot}$, which is 1 dex below the local SFR- $L_{[\text{C II}]}$ relations. The results are consistent with predictions for low-metallicity galaxies at $z > 6$, however, other effects could also play a role in terms of decreasing $L_{[\text{C II}]}$. The detection of A383-5.1 is encouraging and suggests that detections are possible, but much fainter than initially predicted.

Key words: Galaxies: evolution – galaxies: high-redshift – galaxies: ISM – galaxies: formation – submillimetre: galaxies

1 INTRODUCTION

During the past decade, the number of galaxies with measured redshifts $z > 6$ has increased significantly (e.g. Hu et al. 2002; Iye et al. 2006) with even a few spectroscopic redshifts of $z > 7$ (Vanzella et al. 2011; Ono et al. 2012; Schenker et al. 2012; Shibuya et al. 2012; Finkelstein et al. 2013; Watson et al. 2015; Oesch et al. 2015; Zitrin et al. 2015), demonstrating the tremendous potential for progress of our understanding of galaxy formation during the first billion years after the Big Bang. There is an even larger number of galaxies with photometric redshifts $z > 6$ (e.g. McLure et al. 2013; Smit et al. 2015), however, spectroscopic redshifts are essential for studying the physical properties of the interstellar medium and the gas that fuels the star formation. Because of the intrinsic high luminosity and the large gas masses, several starburst and quasar host galaxies have been studied in great detail at $z > 6$ (e.g. Maiolino et al. 2005; Venemans et al. 2012; Wang et al. 2013; Riechers et al. 2013; Willott et al. 2015a; Bañados et al. 2015; Ciccone et al. 2015;

Venemans et al. 2015). Such galaxies are interesting to understand the evolution of the most massive galaxies but are not representative of the overall galaxy population.

Various tracers are used for determining the properties of the gas in star-forming galaxies. In terms of studying molecular gas, CO is most commonly used as it is the second most abundant molecule and with bright emission lines from the rotational transitions that are visible in the (sub-)mm bands. One of the brightest lines seen in the far-infrared (FIR) in local star-forming galaxies is the fine-structure (FS) line [C II] ($^2P_{3/2} \rightarrow ^2P_{1/2}$) at 1900.537 GHz, which is found to correlate with the star formation rate (e.g. De Looze et al. 2014; Sargsyan et al. 2014). While local studies of the FIR FS lines are difficult due to the opacity of the Earth's atmosphere, at high z the lines are shifted towards the (sub-)mm bands and thus observable with ground-based telescopes.

With the increased ground-based capabilities of mm-wavelength telescopes, it has become possible to search for the [C II] line in less extreme galaxies at $z > 6$. However, a clear picture of this line as a tracer of the star formation is not emerging. Recently, Capak et al. (2015) and Willott et al. (2015b) detected [C II]

★ E-mail: kirsten.knudsen@chalmers.se

in bright Lyman-break galaxies (LBG) at $5 < z < 6$ and $z \sim 6.1$, respectively, with the [C II] line luminosities and SFR following similar relations as those found for local star-forming galaxies. The galaxies are UV-luminous ($1-4L^*$; we use L^* for the corresponding redshift), representing the bright end of the UV-luminosity function. Maiolino et al. (2015) targeted three LBGs within the redshift range $z = 6.8 - 7.1$, but did not detect the [C II] line despite the galaxies having estimated SFRs $\sim 5 - 15 M_\odot \text{ yr}^{-1}$. However, they find a detection that is offset from one of the targets possibly explained by feedback and/or gas accretion. Similarly, Schaerer et al. (2015) obtained upper limits for two other LBGs at $z \sim 6.5 - 7.5$, of which one is lensed and with sub- L^* luminosity. Ly α emitting galaxies have been observed, including the massive Ly α -blob ‘Himiko’, however, no confirmed detection has so far been obtained (e.g. Ouchi et al. 2013; Kanekar et al. 2013; Ota et al. 2014; González-López et al. 2014). Almost all of these galaxies have non-detections in the FIR continuum suggesting a low dust-mass. Watson et al. (2015) found a clear detection of dust emission from a spectroscopically confirmed $z = 7.5$ galaxy, however, did not detect an expected bright [C II] line in the frequency range covered. The galaxy is strongly lensed by a magnification factor of 9.5, thus providing constraints on a sub- L^* galaxy.

In this letter we present ALMA observations of [C II] for two sub- L^* galaxies at $z > 6$. The two sources are A383-5.1 ($z = 6.027$) and MS0451-H ($z = 6.703$), which have estimated SFRs of 3.2 and $0.4 M_\odot \text{ yr}^{-1}$, respectively, and estimated magnification factors of $\mu = 11.4 \pm 1.9$ and 100 ± 20 , respectively (Richard et al. 2011; Stark et al. 2015, Kneib et al. in preparation). The strong lensing of both galaxies enables us to probe intrinsically fainter luminosities and SFR than previous observations. We assume a Λ CDM cosmology with $H_0 = 67.3 \text{ km s}^{-1} \text{ Mpc}^{-1}$, $\Omega_M = 0.315$, and $\Omega_\Lambda = 0.685$ (Planck Collaboration et al. 2014).

2 OBSERVATIONS

We observed the sources MS0451-H and A383-5.1 with ALMA in Cycle-2. The observations were carried out in December 2014, January and May 2015. A separate receiver setup was used for each source tuning to the redshifted [C II] line; for A383 at $z = 6.027$ the central frequency was 270.462 GHz and for MS0451-H at $z = 6.703$ it was 246.727 GHz . The correlator was used in the frequency domain mode with one spectral window (spw) having a bandwidth of 1.875 GHz centered on the aforementioned frequencies, and the three other available spw’s used a continuum setup with a bandwidth of 2 GHz each distributed over 128 channels. The telescope configuration has baselines extending between 15 and 350 m for MS0451-H and 15 to 540 m for A383-5.1; the observations include baselines longer than initially proposed for. The integration time was 1.9 hours for MS0451-H and 4.6 hours for A383-5.1. Table 1 summarizes the details of the observations including a list of the calibrators.

Reduction, calibration, and imaging was done using CASA (Common Astronomy Software Application²; McMullin et al. 2007). The pipeline reduced data delivered from the observatory was of sufficient quality, no additional flagging and further calibration was necessary. The pipeline includes the steps required for

Table 1. Summary of the ALMA observations

Date	N_{ant}	Flux	Calibrators Bandpass	Gain
<i>MS0451-H</i>				
10-12-2014	37	J0423-013	J0423-0120	J0501-0159
26-12-2014	40	Uranus	J0338-4008	J0501-0159
26-12-2014	40	Uranus	J0423-013	J0501-0159
<i>A383-5.1</i>				
31-12-2014	36	J0423-013	J0423-0120	J0239-0234
14-01-2015	38	Uranus	J0423-013	J0239-0234
17-01-2015	35	Uranus	J0224+0659	J0239-0234
23-05-2015	34	J0238+166	J0423-013	J0239-0234
23-05-2015	34	J0423-013	J0423-013	J0239-0234
24-05-2015	34	J0238+166	J0224+0659	J0239-0234
24-05-2015	34	J0238+166	J0423-013	J0239-0234

standard reduction and calibration, such as flagging, bandpass calibration, as well as flux and gain calibration. A conservative estimate of the absolute flux calibration is 10%. In the case of A383-5.1, a continuum source, flux density $\sim 2 \text{ mJy}$, is seen 11 arcsec south of the point center. We attempted to self-calibrate using this relatively bright source, however, this did not significantly improve the sensitivity.

The data was imaged both as continuum and spectral cube using natural weighting. A continuum image was produced combining all spectral windows, while a spectral cube was constructed for the spectral window tuned to the redshifted [C II] line. The obtained resolution is $0.86'' \times 0.67''$ PA = 94° for A383-5.1 and $1.6'' \times 0.9''$ PA = 84° , and in both cases the r.m.s. is $11 \mu\text{Jy beam}^{-1}$. The rms in a 15.6 MHz channel near the redshifted line is $0.125 \text{ mJy beam}^{-1}$ and $0.163 \text{ mJy beam}^{-1}$ for A383-5.1 and MS0451-H, respectively.

3 RESULTS

In case of A383-5.1 we detect the redshifted [C II] line. The spectrum is shown in Fig. 1 together with an image of the integrated line overlaid on a near-infrared *HST* F140W image from the CLASH survey³. We fit a Gaussian line profile to the extracted spectrum and use this to derive the line properties. The resulting fit parameters are: central frequency $\nu = 270.4448 \pm 0.0061 \text{ GHz}$, peak flux of $S_{\text{peak}} = 0.96 \pm 0.19 \text{ mJy}$, and FWHM line width of $\Delta V = 100 \pm 23 \text{ km s}^{-1}$. This corresponds to an integrated line intensity $I_{[\text{CII}]} = 0.102 \pm 0.032 \text{ Jy km s}^{-1}$ (including the flux uncertainty added in quadrature). We derive a redshift of $z_{[\text{CII}]} = 6.0274 \pm 0.0002$, which is in agreement with the optical/UV redshift of 6.029 ± 0.002 (Richard et al. 2011) and the C III] redshift of 6.0265 ± 0.00013 (Stark et al. 2015). We note the spectrum has been extracted from a datacube, which was imaged using natural weighting and tapering with 2D Gaussian with a corresponding $1''$ width as the source appears to be marginally extended. Using the uv -data of collapsed spectral channels around the peak of the emission line, we estimate the size of the source to be $\sim 0.16''$ assuming a 2D Gaussian brightness distribution, however, due to the modest signal-to-noise ratio it is difficult to accurately measure its extent. The continuum is not detected, and we place a 5σ upper level $55 \mu\text{Jy}$.

In the field around A383-5.1 we also detect two continuum sources, at 02:48:03.4, -03:31:44.86 with a flux of 2.2 mJy , and at

¹ The setup for A383-5.1 was based on the redshift from Richard et al. (2011), the redshift was revised to 6.029 following observations of the counter-image A383-5.2 (Stark et al. 2015).

² <https://casa.nrao.edu>

³ <https://archive.stsci.edu/prepds/clash/>

02:48:02.8, -03:31:27.67, integrated flux of 0.25 mJy, and an estimated source size of $2.4'' \times 1.1''$ PA = 60° . The former is associated with the cD galaxy of the cluster ($z = 0.188$), and the latter is associated with a spiral galaxy at $z = 0.65$ (denoted B18 in Smith et al. 2001).

For MS0451-H, we do not detect a line, and in Fig. 2 we show the extracted spectrum from the region corresponding to the near-infrared (NIR) source; as for A383-5.1, the spectrum was extracted from a cube that was imaged using natural weighting and tapering. We measure a rms of $0.05 \text{ mJy beam}^{-1}$ for a channel of 100 km s^{-1} . Assuming this corresponds to the FWHM width of the line, we estimate a 5σ upper limit of $0.026 \text{ Jy km s}^{-1}$. We do not detect the continuum and place an upper limit of $55 \mu\text{Jy}$.

We estimate the [C II] line luminosity using $L_{[\text{CII}]} = 1.04 \times 10^{-3} S \Delta V D_L^2 \nu_{\text{obs}}$ (e.g. Solomon & Vanden Bout 2005; Carilli & Walter 2013). De Looze et al. (2014) has investigated the [C II] line as a SFR estimator for local star-forming galaxies against other probes and for different classes of galaxies. We use the relation for low-metallicity galaxies to estimate the SFR from $L_{[\text{CII}]}$ under the assumption that the [C II] line traces star formation in the galaxies. Furthermore, we use the continuum upper limit to estimate the FIR luminosity upper limits assuming a modified blackbody spectrum with a temperature $T = 35 \text{ K}$ and $\beta = 1.6$ (e.g. Rémy-Ruyer et al. 2013). For comparison with the SFR derived from the optical/NIR observations, we estimate an SFR from the L_{IR} assuming a Chabrier IMF (e.g. Carilli & Walter 2013). We correct the values for the estimated gravitational magnification (Richard et al. 2011, Kneib et al., in preparation). Results and upper limits are summarised in Table 2. We note that the CMB temperature is 19.1 K and 21 K for $z = 6.027$ and $z = 6.703$, respectively. Following the analysis of da Cunha et al. (2013), we estimate that the CMB heating would increase the temperature by less than a per cent for the assumed values and that about 14-20% of the intrinsic continuum flux density would be missed due to the CMB background emission.

4 DISCUSSION

A383-5.1 has the lowest [C II] luminosity among all detections of this line at $z > 6$, and the upper limit for MS0451-H is more than 1.5 dex below other upper limits. Both galaxies are selected as UV-bright, star-forming, and with gravitational magnification > 10 . The latter enabled us to do deeper observations than previously presented and thus probe towards SFRs and stellar masses comparable to the low-mass end and less extreme systems. In Fig. 3 we show the results together with results for other high- z and local galaxies.

Using combined stellar population synthesis modeling and photoionization modeling of the gas-component, Stark et al. (2015) finds that the metallicity is $\log(Z/Z_\odot) = -1.33$ for A383-5.1. This relatively low metallicity is comparable to the metallicity found in some nearby dwarf galaxies. The line luminosity for A383-5.1, as well as the MS0451-H upper limit and the IR luminosity limits are similar to nearby, low- Z dwarfs. Using *Herschel* PACS spectroscopy, Cormier et al. (2015) studied the properties of FIR fine-structure lines, including the [C II] line, of the low- Z ISM of dwarf galaxies. The $L_{[\text{CII}]} / L_{\text{IR}}$ ratio has a large scatter for dwarf galaxies, and the lowest metallicity systems, $Z/Z_\odot < 1/20$, agree with that scatter. Based on the $L_{[\text{CII}]}$ of A383-5.1, assuming a ratio of 0.6% and 0.06%, we estimate $L_{\text{IR}} \sim 1.4 - 14 \times 10^9 L_\odot$. This is partly in agreement with the lower limit on the $L_{[\text{CII}]} - L_{\text{FIR}}$ ratio derived from our results (see Table 2), suggesting that the [C II] line contributes

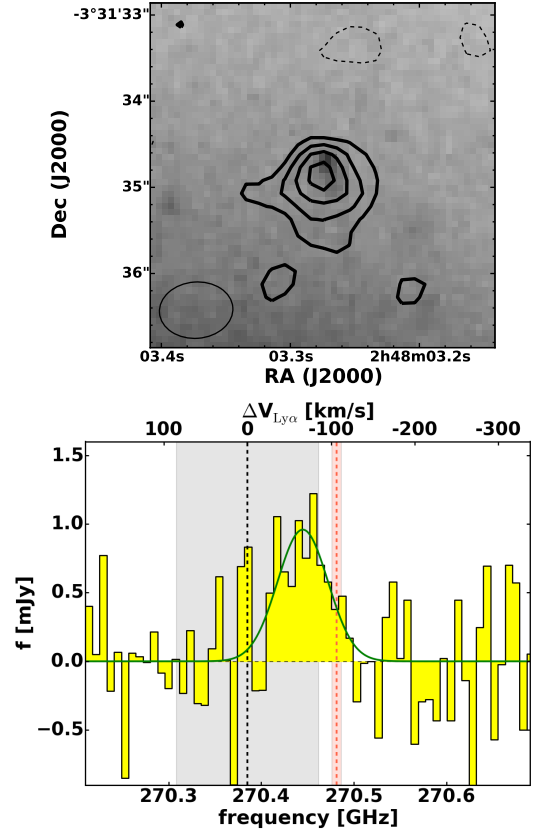


Figure 1. *Top:* HST WFC3 F140W image overlaid with the contours of the integrated spectral line. The contours show 2, 3, 4, 5 σ , and dashed show -2σ . The apparent gradient of NIR emission increasing from the lower part of the image is caused by the bright emission from the central galaxy of the A383 cluster. *Bottom:* ALMA spectra extracted at the position of A383-5.1 and centered at the frequency of the redshifted [C II] line. The green solid curve shows the best-fit Gaussian. The vertical dashed line and grey area shows the corresponding redshift and uncertainty determined from the Ly α line, and the red dashed line and area corresponds to the redshift measured from C III (Stark et al. 2015). The top-axis shows the velocity relative the Ly α redshift.

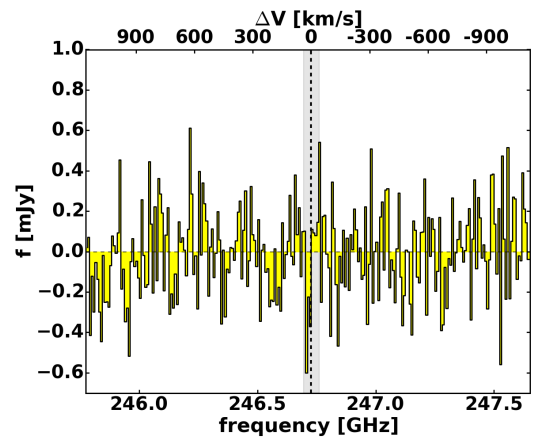


Figure 2. The ALMA band-6 spectrum extracted at the position of the MS0451-H arc. The vertical line and grey area shows indicate the corresponding redshift and uncertainty determined from the Ly α line. The top-axis shows the velocity relative the Ly α redshift.

Table 2. Resulting properties for A383-5.1 and MS0451-H together with UV-optical estimates.

Name	$z_{\text{Ly}\alpha}$	$z_{\text{[CII]}}$	μ	$L_{\text{[CII]}}$ [L_{\odot}]	$\text{SFR}_{\text{[CII]}}$ [$M_{\odot} \text{ yr}^{-1}$]	L_{IR} [L_{\odot}]	SFR_{IR} [$M_{\odot} \text{ yr}^{-1}$]	$\text{SFR}_{\text{optical}}$ [$M_{\odot} \text{ yr}^{-1}$]
A383-5.1	6.029 ± 0.002	6.0274 ± 0.0002	11.4 ± 1.9	$(8.9 \pm 3.1) \times 10^6$ ^a	0.68 ± 0.24	$< 0.5 \times 10^{10}$	< 0.5	3.2
MS0451-H	6.703 ± 0.001	...	100 ± 20	$< 3.0 \times 10^5$ ^b	< 0.04	$< 0.07 \times 10^{10}$	< 0.07	0.4

^a the error includes the uncertainties from the line fit, the flux calibration, and the uncertainty on the magnification.

^b assuming a line width of 100 km s^{-1} as measured for A383-5.1

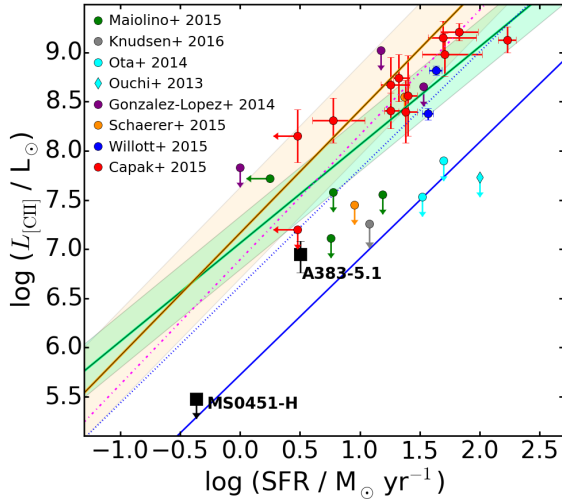


Figure 3. The [C II] line luminosity $L_{\text{[CII]}}$ vs. star formation rate. Black squares show the detection A383-5.1 and the sensitive upper limit for MS0451-H (corrected for magnification). We also include the recent $z \sim 6$ results from Ouchi et al. (2013); Ota et al. (2014); González-López et al. (2014); Willott et al. (2015b); Maiolino et al. (2015); Capak et al. (2015); Schaefer et al. (2015); Knudsen et al. (2016). The $L_{\text{[CII]}}$ - SFR relation, where the green region shows the relation for local star-forming galaxies and the orange region shows that for low-metallicity dwarf galaxies (De Looze et al. 2014). The blue solid and dotted line shows the resulting relation from low-metallicity simulations (Vallini et al. 2015) (solid: $Z = 0.05Z_{\odot}$, dotted: $Z = 0.2Z_{\odot}$) and the magenta dash-dot-line the results for massive $z \sim 2$ galaxies (Olsen et al. 2015).

significantly to the cooling. For MS0451-H, we do not have an estimate for the metallicity given the limited optical (rest-frame UV) data available (Kneib et al., in preparation).

The sample from Capak et al. (2015) contains bright LBGs with luminosities $> L^*$ and in the redshift range $5 < z < 6$, and while this is below the redshift range that we are probing ($z > 6$), it is to date the largest sample of [C II] detections of galaxies that are not quasar host galaxies nor SMGs. That sample is in reasonable agreement with the $\text{SFR}-L_{\text{[CII]}}$ relations seen for local galaxies (e.g. De Looze et al. 2014). Similarly, the two LBG detections from Willott et al. (2015b) also follow these relations. On the other hand, several [C II] searches towards both LAEs and LBGs have resulted in non-detections (Ouchi et al. 2013; Ota et al. 2014; González-López et al. 2014; Maiolino et al. 2015; Schaefer et al. 2015), where several observations provide upper limits below the local $\text{SFR}-L_{\text{[CII]}}$ comparable to our detection of A383-5.1.

With an excitation temperature of 91.2 K and the ionization potential of carbon of 11.2 eV, the [C II] is a good tracer of the diffuse ISM, of the cold neutral medium (CNM) phase as well as of the photon-dominated regions (PDRs) caused by star-formation in

molecular clouds. Both models and observations of nearby galaxies show that [C II] emission is an efficient cooling line and that the line luminosity is correlated with the star-formation rate of galaxies (e.g. De Looze et al. 2014; Sargsyan et al. 2014), however, for IR bright starburst galaxies and AGN, the efficiency drops (e.g. Díaz-Santos et al. 2013).

It is unclear why so many $z > 6$ galaxies remain undetected, or as in the case of A383-5.1, show a fainter than predicted [C II] line. It has been suggested that low metallicity is the main reason. As shown in PDR-modelling, the [C II] line intensity decreases for lower metallicity, although not linearly (e.g. Röllig et al. 2006). Given that the [C II] line correlates well with the SFR for nearby, low-metallicity galaxies (e.g. De Looze et al. 2014), it would be expected that this is also the case for high- z low-metallicity galaxies. However, the [C II] deficit suggests that the physical conditions are very different from nearby low- Z galaxies. This [C II] deficit is different from the classical one found for FIR luminous galaxies (e.g. Luhman et al. 2003; Stacey et al. 2010). Aside from metallicity playing a role, other mechanisms could contribute, such as a harder radiation field which could further ionize the carbon into C^{++} ; in fact the spectral modeling of A383-5.2 (the counterimage) yields a high ionization parameter $\log U = 1.79$ (Stark et al. 2015). In such case, observations of e.g. C III] lines would reveal elevated ratios. Increased temperature of the ISM and PDRs would result in other fine-structure lines being more efficient coolants and thus brighter than [C II]. For example, the [O III] $88 \mu\text{m}$ line is normally expected to be tracing H II regions rather than diffuse and clumpy inter-cloud medium (see e.g. Cormier et al. 2015, for further details). Further, we note that gas-phase carbon could be depleted onto carbonaceous dust grains.

In simulations of high- z galaxies, the recent study by Vallini et al. (2015) focused on differences arising when taking into account varying metallicity. Vallini et al. (2015) produces a metallicity dependent relation for $L_{\text{[CII]}}-\text{SFR}$ based on a constant metallicity distribution throughout the simulated galaxy ($z = 6.6$). For low Z , $Z = 0.05 - 0.2Z_{\odot}$, the relation is below that of local galaxies. A383-5.1 has a metallicity similar to the low- Z assumption of the Vallini et al. (2015) model. The model results are consistent with our detection of A383-5.1, which suggests that metallicity plays an important role. However, given that we only have one detection and the remaining being non-detections, we cannot confirm this. We show the Vallini et al. model results in Fig. 3, and for comparison, include the resulting relation from multi-phase ISM simulations of $z \sim 2$ massive galaxies by Olsen et al. (2015), which tends to follow the relations seen for local galaxies.

It is, however, important to also investigate the selection bias for high- z galaxies. The fact that Lyman- α emitters, despite high estimates for SFR, remain undetected in the relatively deep ALMA observations of the [C II] line, could suggest that SFRs are overestimated and while the Ly- α emission likely traces star formation,

a fraction of it could be powered by other mechanisms, such as shocks of gas inflow.

To summarize, while it has been suggested that [C II] would be a relatively bright tracer for star formation in high- z galaxies – and with the advantage of being redshifted into the ~ 1 mm wavelength range – the recent results show that the line luminosity does not follow the same correlations as local galaxies. With the A383-5.1 detection, we find that it is possible to detect [C II] towards $z > 6$ star-forming galaxies, although the line luminosity is lower than predicted from local galaxies and also from high- z SMGs and QSO hosts. This implies that future observations have the potential to yield detections, although the predicted line flux will likely be lower than when derived from local relations, even when using local low- z relations.

ACKNOWLEDGEMENTS

We thank the staff of the Nordic ALMA Regional Center node for their support and helpful discussions. We thank the referee for useful comments. KK acknowledges support from the Swedish Research Council (grant: 621-2011-5372) and the Knut and Alice Wallenberg Foundation. JR acknowledges support from the ERC starting grant CALENDs (336736). JPK acknowledges support from the ERC advanced grant LIDA and from CNRS. MJ is supported by the Science and Technology Facilities Council [grant number ST/L00075X/1 & ST/F001166/1]. This paper makes use of the following ALMA data: ADS/JAO.ALMA#2013.1.01241.S. ALMA is a partnership of ESO (representing its member states), NSF (USA) and NINS (Japan), together with NRC (Canada) and NSC and ASIAA (Taiwan) and KASI (Republic of Korea), in co-operation with the Republic of Chile. The Joint ALMA Observatory is operated by ESO, AUI/NRAO and NAOJ.

References

Bañados E., Decarli R., Walter F., Venemans B. P., Farina E. P., Fan X., 2015, *ApJ*, **805**, L8
 Capak P. L., et al., 2015, *Nature*, **522**, 455
 Carilli C. L., Walter F., 2013, *ARA&A*, **51**, 105
 Ciccone C., et al., 2015, *A&A*, **574**, A14
 Cormier D., et al., 2015, *A&A*, **578**, A53
 De Looze I., et al., 2014, *A&A*, **568**, A62
 Díaz-Santos T., et al., 2013, *ApJ*, **774**, 68
 Finkelstein S. L., et al., 2013, *Nature*, **502**, 524
 González-López J., et al., 2014, *ApJ*, **784**, 99
 Hu E. M., Cowie L. L., McMahon R. G., Capak P., Iwamuro F., Kneib J.-P., Maihara T., Motohara K., 2002, *ApJ*, **568**, L75
 Iye M., et al., 2006, *Nature*, **443**, 186
 Kanekar N., Wagg J., Ram Chary R., Carilli C. L., 2013, *ApJ*, **771**, L20
 Knudsen K. K., Watson D., Frayer D., Christensen L., Gallazzi A., Michałowski M. J., Richard J., Zavala J., 2016, preprint, ([arXiv:1603.03222](https://arxiv.org/abs/1603.03222))
 Luhman M. L., Satyapal S., Fischer J., Wolfire M. G., Sturm E., Dudley C. C., Lutz D., Genzel R., 2003, *ApJ*, **594**, 758
 Maiolino R., et al., 2005, *A&A*, **440**, L51
 Maiolino R., et al., 2015, *MNRAS*, **452**, 54
 McLure R. J., et al., 2013, *MNRAS*, **432**, 2696
 McMullin J. P., Waters B., Schiebel D., Young W., Golap K., 2007, in Shaw R. A., Hill F., Bell D. J., eds, *Astronomical Society of the Pacific Conference Series Vol. 376, Astronomical Data Analysis Software and Systems XVI*. p. 127
 Oesch P. A., et al., 2015, *ApJ*, **804**, L30

Olsen K. P., Greve T. R., Narayanan D., Thompson R., Toft S., Brinch C., 2015, *ApJ*, **814**, 76
 Ono Y., et al., 2012, *ApJ*, **744**, 83
 Ota K., et al., 2014, *ApJ*, **792**, 34
 Ouchi M., et al., 2013, *ApJ*, **778**, 102
 Planck Collaboration et al., 2014, *A&A*, **571**, A16
 Rémy-Ruyer A., et al., 2013, *A&A*, **557**, A95
 Richard J., Kneib J.-P., Ebeling H., Stark D. P., Egami E., Fiedler A. K., 2011, *MNRAS*, **414**, L31
 Riechers D. A., et al., 2013, *Nature*, **496**, 329
 Röllig M., Ossenkopf V., Jeyakumar S., Stutzki J., Sternberg A., 2006, *A&A*, **451**, 917
 Sargsyan L., Samsonyan A., Lebouteiller V., Weedman D., Barry D., Bernard-Salas J., Houck J., Spoon H., 2014, *ApJ*, **790**, 15
 Schaerer D., Boone F., Zamojski M., Staguhn J., Dessauges-Zavadsky M., Finkelstein S., Combes F., 2015, *A&A*, **574**, A19
 Schenker M. A., Stark D. P., Ellis R. S., Robertson B. E., Dunlop J. S., McLure R. J., Kneib J.-P., Richard J., 2012, *ApJ*, **744**, 179
 Shibuya T., Kashikawa N., Ota K., Iye M., Ouchi M., Furusawa H., Shimasaku K., Hattori T., 2012, *ApJ*, **752**, 114
 Smit R., et al., 2015, *ApJ*, **801**, 122
 Smith G. P., Kneib J.-P., Ebeling H., Czoske O., Smail I., 2001, *ApJ*, **552**, 493
 Solomon P. M., Vanden Bout P. A., 2005, *ARA&A*, **43**, 677
 Stacey G. J., Hailey-Dunsheath S., Ferkinhoff C., Nikola T., Parshley S. C., Benford D. J., Staguhn J. G., Fiolet N., 2010, *ApJ*, **724**, 957
 Stark D. P., et al., 2015, *MNRAS*, **450**, 1846
 Vallini L., Gallerani S., Ferrara A., Pallottini A., Yue B., 2015, *ApJ*, **813**, 36
 Vanzella E., et al., 2011, *ApJ*, **730**, L35
 Venemans B. P., et al., 2012, *ApJ*, **751**, L25
 Venemans B. P., Walter F., Zschaechner L., Decarli R., De Rosa G., Findlay J. R., McMahon R. G., Sutherland W. J., 2015, *ApJ* in press, [arxiv:1511.07432](https://arxiv.org/abs/1511.07432),
 Wang R., et al., 2013, *ApJ*, **773**, 44
 Watson D., Christensen L., Knudsen K. K., Richard J., Gallazzi A., Michałowski M. J., 2015, *Nature*, **519**, 327
 Willott C. J., Bergeron J., Omont A., 2015a, *ApJ*, **801**, 123
 Willott C. J., Carilli C. L., Wagg J., Wang R., 2015b, *ApJ*, **807**, 180
 Zitrin A., et al., 2015, *ApJ*, **810**, L12
 da Cunha E., et al., 2013, *ApJ*, **765**, 9

This paper has been typeset from a \LaTeX file prepared by the author.